

Small-scale recombination He – Sr⁺(Ca⁺) lasers

E L Latush, G D Chebotarev, M F Sem

Abstract. A review of specific features and output characteristics of small-scale ($l \leq 30$ cm, $d \leq 1.1$ cm) gas-discharge recombination He – Sr⁺ ($\lambda = 430.5$ nm) and He – Ca⁺ ($\lambda = 373.7$ nm) lasers is provided. Such compact lasers are characterised by a relatively high reliability and durability. These lasers are easy to operate and are capable of generating laser pulses with high repetition rates f , a high specific mean power P_{sp} , and an improved quality of output radiation. A typical mean power P of self-heating sealed-off He – Sr⁺ (Ca⁺) laser tubes with $l \approx 30$ cm and $d \approx 1$ cm is ~ 0.5 W. The best specific characteristics of a He – Sr⁺ laser with tubes of this type were achieved with $l = 20$ cm and $d = 0.6$ cm ($P_{sp} = 73$ mW cm⁻³) and $l = 9$ cm and $d = 0.55$ cm ($P_{sp} = 65$ W cm⁻³). The best specific characteristics for a He – Ca⁺ laser were achieved with $l = 26.5$ cm and $d = 0.7$ cm ($P_{sp} = 50$ mW cm⁻³). The use of forced water cooling in a He – Sr⁺ (Ca⁺) laser allowed the powers $P = 3.9$ W and $P_{sp} = 137$ mW cm⁻³ to be achieved with a tube with $l = 30$ cm and $d = 1.1$ cm for $f = 29$ kHz. A new method of inputting metal vapours based on cataphoresis is considered in detail. Using this method allowed the output characteristics of a He – Sr⁺ laser to be considerably improved and a record specific power $P_{sp} = 277$ mW cm⁻³ to be achieved for a tube with $l = 26$ cm and $d = 0.3$ cm with $f = 30$ kHz and $P = 510$ mW. A record gain, 0.15 cm⁻¹, was also achieved under these conditions. Some possible areas of applications of small-scale He – Sr⁺ (Ca⁺) lasers in semiconductor microtechnology, holography, ecology, and medicine are outlined.

1. Introduction

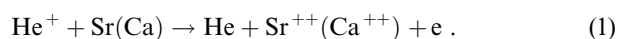
Ion recombination lasers using strontium and calcium vapours generate radiation on the $6^2S_{1/2} - 5^2P_{3/2,1/2}^o$ transitions of SrII ($\lambda = 430.5$ and 416.2 nm) and $5^2S_{1/2} - 4^2P_{3/2,1/2}^o$ transitions of CaII ($\lambda = 373.7$ and 370.6 nm) in the afterglow of a pulse-periodic longitudinal discharge in mixtures of vapours of these metals with helium at pressures close to the atmospheric pressure or higher. Observation of lasing for these transitions was reported for the first time in papers [1, 2], where the recombination mechanism of pumping of these lasers was proposed. A more detailed discussion

of this pumping mechanism was provided in Refs [3, 4], where the main specific features of lasing in recombination lasers were determined, the general principles of searching for population inversion under conditions of recombination – collisional kinetics were formulated, and some new recombination laser transitions in vapours of other metals were found. These studies stimulated more detailed research into the properties of recombination metal-vapour lasers (MVLs), which was carried out by our group and several other groups in Russia and abroad. The main results of these studies are summarised in monographs [5–7] and reviews [8–11].

Although lasing in the recombination regime was observed for many laser transitions in vapours of different metals, lasers using strontium and calcium vapours, emitting radiation in the violet and UV spectral ranges, were found to be especially efficient due to the fact that the arrangement of laser and adjacent energy levels in these systems is especially favourable for the creation of population inversion in a dense recombining gas-discharge plasma. Therefore, the main efforts of researchers were concentrated on improving the parameters of output radiation of He – Sr⁺ (Ca⁺) lasers. In addition, these lasers emit in the short-wavelength spectral range, which is deficient in simple and reliable laser sources.

The spectra of SrII and CaII have a similar arrangement of energy levels. Therefore these lasers are characterised by similar lasing conditions and output characteristics. The lines with $\lambda = 430.5$ and 416.2 nm in SrII and the lines with $\lambda = 373.7$ and 370.6 nm in CaII correspond to a strong and a weak component in doublets and have a common upper level. Due to the competition of transitions in a nonselective cavity, lasing occurs only through strong components of these doublets (430.5 nm in SrII and 373.7 nm in CaII). By suppressing these components, one can also achieve a considerable lasing power for the lines with $\lambda = 416.2$ and 370.6 nm.

Briefly, the mechanism of lasing in these lasers can be described in the following way. A discharge current pulse gives rise to an almost complete double ionisation of metal atoms due to an electron impact in a mixture of strontium or calcium vapours (~ 0.1 Torr) with helium ($\sim 400 - 700$ Torr). Low potentials of single and double ionisation of these metals promote this process. The sum of these potentials is equal to 16.72 eV for Sr and 17.98 eV for calcium, which is much less than the potential of single ionisation for helium (24.58 eV). In addition, Sr⁺⁺ and Ca⁺⁺ ions are generated through recharging accompanied by double ionisation [1, 2, 12]:



This process occurs not only within the current pulse, but also in the discharge afterglow.

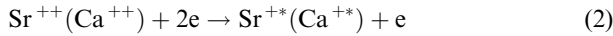
E L Latush, G D Chebotarev, M F Sem Department of Physics, Rostov State University, ul. Zorge 5, 344090 Rostov-on-Don, Russia
e-mail: latush@phys.rnd.runnet.ru

Received 12 January 2000

Kvantovaya Elektronika 30 (6) 471–478 (2000)

Translated by A M Zheltikov, edited by M N Sapozhnikov

In the regime optimal for lasing, the contribution of this reaction into ionisation may range from 10 to 20%. When the discharge current is switched off and electrons are cooled down to a temperature $T_e \approx 0.5 - 0.3$ eV, three-body electron–ion recombination



begins to play an important role, populating excited levels of ions. The recombination flux related to optical and electron–collisional transitions (electron de-excitation) populates the upper laser level through a cascade process. On the other hand, electron de-excitation of the lower laser level results in a fast population transfer to the 2D metastable level and to the ground state of metal ions.

Thus, recombination is the main mechanism behind the pumping of levels, while electron de-excitation is a crucial factor in the creation of population inversion. Both of these processes become efficient when T_e is low. Therefore, recombination lasers efficiently operate at high helium pressures p_{He} . Elastic collisions with atoms of this light rare gas in a discharge afterglow result in the rapid cooling of electrons.

For helium pressures of the order of the atmospheric pressure, the duration of recombination of doubly charged strontium and calcium ions is very small ($\sim 0.2 - 0.3$ μs). The duration of a lasing pulse is the same or somewhat smaller. As demonstrated by experiments with doubled current pulses [4] and pulse trains [13], the repetition rates f of laser pulses produced in He – Sr⁺ (Ca⁺) lasers may be very high (~ 1 MHz). The limitations on f may stem only from thermal factors. Therefore, pulse repetition rates $f = 5 - 10$ kHz can be achieved in reality in the pulsed–periodic regime without forced cooling.

Investigations in this direction have demonstrated that He – Sr⁺ (Ca⁺) lasers are capable of generating radiation with a mean power P up to several watts, the efficiency $\eta \approx 0.1\%$, and the gain of the active medium $\kappa_0 = 0.05 - 0.1$ cm^{-1} [5, 6]. The mean power P was increased by the following methods: an increase in the active length l up to 0.9 m [14] and the inner diameter of the discharge tube d up to 4 cm [15, 16], an increase in the repetition rate f with simultaneous intensification of heat removal due to air [17] and water [18] cooling, and a blackening of the tube [19] or the use of segmented laser tubes, where pieces of metal were removed from the discharge area [5, 6]. Self-heating of a medium due to the discharge in the active area of the tube was employed in virtually all cases.

In this paper, we will focus on the investigation of small-scale He – Sr⁺ (Ca⁺) lasers with $l \leq 30$ cm and $d \leq 1.1$ cm. The tubes in such lasers are usually characterised by a high reliability and durability. These tubes are easy to fabricate and convenient in exploitation. Importantly, He – Sr⁺ (Ca⁺) lasers usually require high discharge voltages, which necessitates high pressures p_{He} . Decreasing the sizes of a tube, one can lower the voltages applied to the tube and discharge currents. Small-diameter tubes allow the mode structure of radiation to be improved. Due to the increase in the efficiency of the removal of excessive heat from the discharge area to the tube walls, such tubes also usually permit one to increase the pulse repetition rate f . As a consequence, output radiation with a power of several hundreds of milliwatts can be generated in spite of small sizes of the tube. This level of output radiation powers is sufficient for many applications.

Below, we systematise the results of earlier studies devoted to small-scale He – Sr⁺ (Ca⁺) lasers and present

the results of some recent investigations on this subject that have not been analysed in reviews on recombination lasers before.

2. Ways of achieving high mean radiation powers

Consider the factors that may allow us to keep sufficiently high P in spite of the decrease in l and d . First, we can increase the pulse repetition rate, thus compensating for the lowering in the lasing energy \mathcal{E} of each pulse. We can also attempt to employ the regimes of He – Sr⁺ (Ca⁺) lasers with pressures p_{He} exceeding the atmospheric pressure. However, the latter approach makes the design of the tube more complicated and requires high voltages. Note also that, as d decreases, the use of pieces of evaporated metal in the tube channel becomes less convenient because such pieces partially block the optical aperture of the channel. Therefore, it is desirable to remove the pieces of metal from the discharge area in this case.

The heat exchange in He – Sr⁺ (Ca⁺) lasers with an open ceramic tube (Fig. 1a) or a tube placed inside a glass or quartz shell (Fig. 1b) is adequately described by the relation [19]

$$Q = Q_1 + Q_2 = l[0.0277(T + T_a)^{0.2}(T - T_a)^{1.25}d_1^{0.75} + 1.78 \times 10^{-9}d_1\epsilon T^4], \quad (3)$$

where l is the length in metres, Q is the thermal loss power in watts, d_1 is the outer diameter of a ceramic discharge tube in centimetres, T and T_a are the temperatures of the tube wall and the ambient air in Kelvin degrees, and ϵ is the blackening degree of the tube surface ($\epsilon \approx 0.5$ for BeO ceramics). The first term Q_1 in (3) describes heat losses due to convective heat exchange, while the second term Q_2 governs heat losses due to thermal emission. If the pieces of metal are placed in the discharge channel, then T is determined by the optimal vapour pressure: $T \approx 860 - 900$ K for strontium and $T \approx 890 - 940$ K for calcium. The magnitude of radiative losses is $\sim 70\%$ of the total magnitude of heat losses at such temperatures. The total magnitude of heat losses under these conditions is, in fact, equal to the mean power deposited in

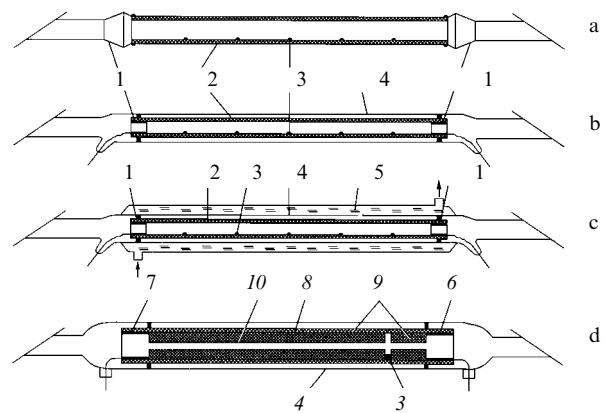


Figure 1. Active elements of He – Sr⁺ (Ca⁺) lasers (1) electrodes, (2) ceramic (usually BeO ceramic) discharge tube, (3) pieces of strontium or calcium, (4) outer glass or quartz shell, (5) housing of water cooling, (6) anode, (7) cathode, (8) outer BeO tube, (9) inner BeO tube, and (10) active discharge area of a cataphoresis laser.

the tube. Thus, this quantity and the lasing efficiency determine the mean power of lasing $P = \eta Q$.

One can see from formula (3) that there are several ways of increasing P : (a) One can increase ε up to $\sim 0.9 - 1.0$ by blackening the tube surface; (b) one can increase the outer diameter of the ceramic tube, keeping the inner diameter small (this is a consequence of a high thermal conductivity of BeO ceramics, which leads to a few Kelvin degree difference between the temperatures of the exterior and interior ceramic surfaces); (c) one can use forced air or water cooling instead of free convective cooling; and (d) one can remove a metal from the inner surface of the discharge channel and deliver a metal vapour with a concentration required for the optimal lasing regime to the tube, which would make the temperature of the walls independent of the vapour pressure. An additional advantage of the latter approach is that it simultaneously prevents the blocking of the aperture of the optical channel by pieces of strontium or calcium.

We should keep in mind, however, that the repetition rate f in the pulse-periodic regime is limited because of the overheating of the active medium in near-axis parts of the tube. Analysis of this factor shows [18] that the limiting optimal pulse repetition rate for a He – Sr⁺ (Ca⁺) laser (in kilohertz) is given by

$$f_{\text{opt}} \leq \frac{55}{d^2}, \quad (4)$$

where d is measured in centimetres. Fortunately, the limiting value of f_{opt} is high for small-diameter tubes, and such repetition rates are usually not achieved because of other limiting factors.

Using formula (3), we can write simplified expressions for Q and P :

$$Q \approx (Ad_1^{0.75} + Bd_1)l \sim ld_1, \quad (5)$$

$$P = Q\eta \approx (Ad_1^{0.75} + Bd_1)l\eta \sim ld_1\eta. \quad (6)$$

If the pieces of metal are placed in a discharge tube in the regime of self-heating, parameters A and B remain approximately constant, because the temperature of the interior surface of tubes is determined by the pressure of metal vapour required for optimal lasing, changing within a narrow range even for large variations in p_{He} . Generally, A and B depend on T . In carefully optimised systems, the lasing efficiency may usually reach $\sim 0.1\%$ in the case of a He – Sr⁺ laser and approximately 0.07% in the case of a He – Ca⁺ laser.

The specific mean power for cylindrical tubes can be found from Eqn (6):

$$P_{\text{sp}} = \frac{P}{V_a} \frac{\eta(Ad_1^{0.75} + Bd_1)}{(\pi d^2/4)} \sim \frac{d_1}{d^2}, \quad (7)$$

where V_a is the active volume. We emphasise that the denominator in Eqn (7) involves the inner diameter of the tube, while the numerator involves the outer diameter.

On the other hand, the quantities P and P_{sp} can be expressed in terms of the specific energy \mathcal{E}_{sp} of a laser pulse:

$$P_{\text{sp}} = f\mathcal{E}_{\text{sp}} \sim f, \quad P = f\mathcal{E}_{\text{sp}}V_a. \quad (8)$$

Assuming that \mathcal{E}_{sp} is virtually independent of d for given p_{He} , we can apply Eqns (7) and (8) to find that

$$f \sim d_1/d^2. \quad (9)$$

Thus formulas (7)–(9) indicate that, with a fixed outer diam-

eter of a tube, one can expect an abrupt increase in P_{sp} and f with the decrease in the inner diameter, while in accordance with Eqn (6), the power P should remain unchanged.

A more detailed analysis of this problem can be performed using optimal-scaling relations derived in our papers [11, 20].

3. The types of small-scale He – Sr⁺(Ca⁺) lasers

The main parameters, operation conditions, and the attainable output characteristics of small-scale He – Sr⁺ (Ca⁺) lasers are summarised in Table 1. For comparison, this table also presents parameters of a typical He – Sr⁺ laser with a medium-size tube ($d = 1.5$ cm and $l = 40$ cm). Consider the specific features of each of the lasers mentioned in the table.

Tube 1 is one of the first of our self-heating units with a thin-wall BeO ceramic discharge tube placed in a molybdenum glass shell (Fig. 1b). Pieces of strontium are placed on the interior surface of ceramics. The tube was optimised and sealed off. Being employed in this way, this tube has shown a reasonable durability for many years, displaying stable energy characteristics whenever it was switched on even after very large periods of time. Getters were not employed in this tube. The functions of getters were performed by a strontium vapour. The heating of strontium resulted in the self-cleaning of the discharge from the air and other molecular impurities, leading to the establishment of a laser regime with $f \approx 6$ kHz and $P = 500 - 600$ mW. The time of self-heating was as short as 5–10 min. Parameters and the design of a similar, but longer tube ($l = 50$ cm, $d = 1.1$ cm, and $P = 1$ W) are described in greater detail in [21].

Tube 2 had a similar design but employed ceramics with thicker walls ($d_1 = 1.6$ cm and $d = 1$ cm). In accordance with Eqns (7) and (9), this tube allowed f and P_{sp} to be increased and the power $P = 630$ mW to be achieved in spite of the decrease in V_a by a factor of nearly 1.5.

Even better specific parameters were achieved with tubes 3 and 4 [22]. Tube no. 3 allowed the specific mean power $P_{\text{sp}} = 73$ mW cm⁻³, which is the highest specific mean power for self-heating He – Sr⁺ lasers, and a comparatively high mean power $P = 205$ mW to be achieved with $V_{\text{opt}} \sim 3$ cm³. Note that the gain α_0 under these conditions was as high as 0.14 cm⁻¹, which is approximately two times higher than the typical gains ($0.06 - 0.08$ cm⁻¹). Approximately the same specific power, $P_{\text{sp}} = 65$ mW cm⁻³, was obtained in the shortest tube 4 with $l = 9$ cm and $d = 0.55$ cm. The volume of this tube V_{opt} was as low as ~ 1 cm³. However, the power P was as high as 70 mW in this case, which is sufficient for many applications.

A self-heating sealed-off He – Ca⁺ laser tube 5, which was similar in its design to the He – Sr⁺ tube 1, had virtually the same durability, reliability, and maintenance characteristics as tube 1. Tube 5 was capable of generating radiation at the 373.7 nm UV line of CaII with a power $P = 450$ mW, which is only 25% less than the power of radiation produced by the He – Sr⁺ tube 1 at 430.5 nm. A laser with tube 6 with thicker walls ($d_1 = 1.2$ cm and $d = 0.7$ cm) has allowed a specific mean power $P_{\text{sp}} = 50$ mW cm⁻³, which is a record specific mean power for He – Ca⁺ lasers, to be achieved.

Our studies [3–6] of recombination He – Sr⁺ (Ca⁺) lasers have demonstrated that the energy of laser pulses

Table.1 Small-scale He – Sr⁺ (Ca⁺).

| Type of laser | λ/nm | Tube number | l/cm | d_1/cm | $d(d_{\text{opt}})/\text{cm}$ | $V_a(V_{\text{opt}})/\text{cm}^3$ | f/kHz | P/mW | $P_{\text{sp}}(P_{\text{sp}}^{\text{opt}})/\text{mW cm}^{-3}$ | $\mathcal{E}/\mu\text{J}$ | $\mathcal{E}_{\text{sp}}(\mathcal{E}_{\text{sp}}^{\text{opt}})/\mu\text{J cm}^{-3}$ | P_{pk}/W | $\eta(\eta_{\text{opt}})/\%$ | $p_{\text{He}}/\text{Torr}$ | Comments | Refs |
|---|---------------------|-------------|---------------|-----------------|-------------------------------|-----------------------------------|----------------|---------------|---|---------------------------|---|--------------------------|------------------------------|-----------------------------|---|-----------|
| Self-heating He – Sr ⁺ laser | 430.5 | 1 | 30 | 1.4 | 1.1(1.0) | 28.5(23.5) | 6 | 600 | 21(26) | 100 | 3.5(4.6) | 500 | 0.1(0.12) | 600 | Large service lifetime | [5, 21] |
| | | 2 | 25 | 1.6 | 1.0(0.9) | 19.6(15.9) | 8 | 630 | 32(40) | 78.8 | 4.0(5.0) | 394 | 0.08(0.1) | 684 | – | This work |
| | | 3 | 20 | 0.8 | 0.6(0.42) | 5.66(2.83) | 10 | 205 | 37(73) | 20.5 | 3.6(7.3) | 103 | 0.06(0.12) | 608 | $\kappa_0 = 0.14 \text{ cm}^{-1}$ | [22] |
| | | 4 | 9 | 1.0 | 0.55(0.39) | 2.14(1.07) | 18 | 70 | 33(65) | 3.9 | 1.8(3.6) | 19.5 | 0.04(0.08) | 684 | The shortest tube | [22] |
| Self-heating He – Ca ⁺ laser | 373.7 | 5 | 30 | 1.4 | 1.1(1.0) | 28.5(23.5) | 6.5 | 450 | 16(19) | 70 | 2.5(3.0) | 350 | 0.07(0.08) | 700 | – | [5, 21] |
| | | 6 | 26.5 | 1.2 | 0.7(0.57) | 10.2(6.8) | 9.5 | 340 | 33(50) | 36 | 3.5(5.3) | 143 | 0.04(0.06) | 456 | Thick-wall tube | this work |
| He – Sr ⁺ laser with a high pressure of helium | 430.5 | 7 | 20 | 1.5 | 0.8(0.3) | 10(1.4) | 3.2 | 62 | 6.2(44) | 19 | 1.9(14) | 250 | –(0.06) | 3000 | Helium circulation | [23] |
| Air-cooled He – Sr ⁺ laser | 430.5 | 8 | 20 | 1.2 | 0.7(0.55) | 7.7(4.8) | 15 | 350 | 45(73) | 23 | 3(4.8) | 90 | 0.06(0.1) | 500 | – | [27] |
| Water-cooled He – Sr ⁺ laser | 430.5 | 9 | 30 | 1.4 | 1.1(1.0) | 28.5(23.5) | 29 | 3900 | 137(166) | 134 | 4.7(5.7) | 650 | 0.12(0.14) | 500 | The thickness of the helium layer $\Delta = 0.5 \text{ mm}$ | [5, 18] |
| Cataphoresis He – Sr ⁺ laser | 430.5 | 10 | 26 | 1.1 | 0.3 | 1.84 | 30 | 510 | 277 | 17 | 9.2 | 85 | 0.06 | 608 | $\kappa_0 = 0.15 \text{ cm}^{-1}$ | [28, 29] |
| Typical mediumsize He – Sr ⁺ laser | 430.5 | 11 | 40 | 2.4 | 1.5 | 70.7 | 5 | 1200 | 17 | 240 | 3.4 | 1200 | 0.12 | 560 | – | [5, 6] |

Note: Parameters in parentheses (the effective optical diameter d_{opt} and the effective active volume V_{opt} , as well as the specific power $P_{\text{sp}}^{\text{opt}}$, the lasing pulse energy $\mathcal{E}_{\text{sp}}^{\text{opt}}$, and the efficiency η_{opt} calculated for V_{opt}) include the blocking of the tube channel with pieces of metal and the electrodes.

increases with increasing p_{He} in these lasers. The optimal pressure of a metal vapour also increases under these conditions. However, the range of pressures $p_{\text{He}} > 1 \text{ atm}$ is usually inaccessible in tubes with a longitudinal discharge with a typical length $l \approx 40 - 50 \text{ cm}$, because high voltages are required in this case and uncontrollable evaporation accompanying discharge breakdown on a piece of metal, especially during the heating of the tube. At the same time, the studies of a transverse discharge [24–26] have shown that the increase in the energy of laser pulses produced by He – Sr⁺ (Ca⁺) lasers does not saturate for pressures up to at least $p_{\text{He}} \approx 1.5 \text{ atm}$.

To determine the limiting output characteristics of He – Sr⁺ (Ca⁺) lasers that can be achieved by increasing the pressure of the mixture, we performed experiments [23] aimed at measuring the pressure p_{He} corresponding to the saturation of the output laser power. To carry out such measurements, we used a longitudinal-discharge tube 7, which was

made of BeO ceramics and which had a comparatively small length ($l = 20 \text{ cm}$ and $d = 8 \text{ mm}$). This tube was placed inside a thick-wall quartz shell. A strontium vapour was produced using a generator, which was heated with a separate oven and which was located near the anode end of the tube.

A vapour was delivered by means of slow helium pumping, which allowed discharge breakdown on strontium pieces to be avoided and a uniform distribution of vapour along the active length to be achieved. Experimental studies have shown that the maximum values of P and \mathcal{E} are achieved for $p_{\text{He}} \approx 4 \text{ atm}$. The specific energy of laser pulses $\mathcal{E}_{\text{sp}} \approx 14 \mu\text{J cm}^{-3}$ achieved in these experiments is a record value of this parameter for longitudinal-discharge lasers of this type. A high specific peak power, $P_{\text{sp}}^{\text{pk}} \approx 180 \text{ W cm}^{-3}$, achieved for this laser is due to the fact that the laser pulse is shortened from 200–300 ns (for $p_{\text{He}} \approx 1 \text{ atm}$) down to $\sim 80 \text{ ns}$ (for $p_{\text{He}} \approx 4 \text{ atm}$). In the case of tubes where a Sr (Ca) vapour is produced due to self-heating, the maximum

mean powers are usually achieved when the pressure p_{He} approaches the atmospheric pressure [5, 22].

Tubes 8 and 9 employed forced air and water cooling, respectively. Laser tube no. 8, which was investigated in our laboratory [27], included an open BeO ceramic element (Fig. 1a) covered with a cylindrical glass housing with several side inlets and outlets for the air flow. With $p_{\text{He}} = 500$ Torr, the values of f and P were increased from 5 kHz and 150 mW (characteristic values of these parameters in the absence of air flow) up to 15 kHz and 350 mW (in the case of a maximum air flow). The lasing efficiency remained virtually unchanged in this case, $\eta \approx 0.1\%$.

The deviation of the power growth from a proportional behaviour with the increase in f is due to the decrease in the effective active length because of the inhomogeneity of tube cooling in the case of maximum flow rates. The power P_{sp} was as high as 73 mW cm^{-3} in this regime. A He – Sr⁺ laser with air cooling was also studied in [17], where a tube made of alumina ceramics with $d = 1.26$ cm, $d_1 = 1.8$ cm, and $l = 60$ cm was placed inside an intimately mating quartz housing and was cooled by an air flow from five fans located on the side of the tube. The power P was increased by a factor of 1.4 under these conditions.

A more radical improvement of parameters of laser radiation was achieved in our experiments with water cooling [18, 19], although the use of water cooling in metal-vapour lasers encounters certain difficulties associated with the necessity of sustaining high temperatures of walls in a discharge tube. In the case of He – Sr⁺ (Ca⁺) lasers, this temperature is about ~ 600 °C. In addition, beryllium oxide has a high thermal conductivity. Therefore, one has to avoid direct contact of water with ceramics, because inadequately high powers of a pump source would be otherwise required to ensure the required temperature difference between the interior and exterior surfaces of ceramics (~ 500 °C).

The aforesaid explains why a thermal resistance should be introduced. A layer of helium and quartz played the role of such a resistance in our water-cooled tubes. In other words, water was used to cool the quartz housing, and heat was transferred through quartz and a helium layer between the housing and the ceramic tube [18, 19]. If the power of the pump source and the admissible repetition rate f are given, we can choose the thickness Δ of the helium layer in such a way as to ensure that the heat removal due to water cooling is optimal in terms of the required vapour pressure and the efficiency of using the power of the power-supply source. Fortunately, due to the high thermal conductivity of helium, the required value of Δ is not too small.

The dependences presented in Refs [5, 6, 19] indicate that Q drastically increases for $\Delta \leq 1$ mm. In order to ensure uniform heat removal, one has to calibrate these small values of Δ very carefully. However, as mentioned above, f cannot be increased infinitely through the intensification of heat removal from the exterior surface of a laser tube because of the overheating of near-axis discharge areas. The temperature $T \approx 2300$ K is critical for the elimination of population inversion. Nevertheless, the results of calculations performed in [5, 6, 18, 19] reveal a considerable resource for the increase in the mean lasing power due to the growth in f with simultaneous intensification of heat removal.

Our experiments [18, 19] with a small-scale active element of a water-cooled He – Sr⁺ laser employed a BeO ceramic discharge tube (Fig. 1c) with $d = 1.1$ cm, $d_1 = 1.4$ cm, and $l = 30$ cm. The available set of quartz tubes allowed us to

vary the thickness of a helium layer from 0.5 to 1.5 mm. The mean power of laser radiation without water cooling in the optimal regime was $P \approx 600$ mW for $f = 6$ kHz. The use of water cooling permitted the repetition rate f to be increased: for $\Delta = 1.5$ mm, we had $f = 11$ kHz, $P = 1.2$ W, and $P_{\text{sp}} = 42 \text{ mW cm}^{-3}$ [19], while for $\Delta = 0.5$ mm, the repetition rate was as high as 29 kHz, and the powers were $P = 3.9$ W and $P_{\text{sp}} = 137 \text{ mW cm}^{-3}$ [18]. Note that the mean power $P = 3.9$ W, achieved in these experiments, remains a record value for He – Sr⁺ lasers up to now, while the specific power attainable with such lasers is several times higher than the specific powers that can be achieved with standard laser tubes.

These encouraging results initiated a joint research project aimed at investigating a He – Sr⁺ laser. This joint research included studies performed in 1991 by C E Little and T R Pugsley and E L Latush at St Andrews University (UK) [7]. These experiments were performed with a BeO ceramic tube with a rectangular (8 mm × 24 mm) discharge channel and a cylindrical exterior surface ($d_1 = 31$ mm and $l = 40$ cm). The tube was placed inside a quartz housing of a water-cooling system with a variable gap between the ceramic tube and the housing.

In the absence of water cooling, this tube allowed the output power $P = 1$ W to be achieved in the optimal regime with a power consumed from a rectifier equal to $P_{\text{in}} = 1$ kW and $f \approx 4.5$ kHz. The use of a tube with water-cooling system with $\Delta = 2$ mm permitted the improvement of the output parameters of laser radiation: $P = 2.3$ W, $P_{\text{in}} = 2.5$ kW, and $f \approx 10$ kHz. With smaller gaps, the operation of the tube was unstable, and it was difficult to reach the lasing threshold because of the insufficient power of the power-supply unit.

Experiments performed with water-cooled small-scale tubes have shown that the use of thermal-resistance gaps whose thickness is not extremely small ($\Delta \approx 1 - 2$ mm) may ensure a long-term stability of small-scale He – Sr⁺ (Ca⁺) lasers with a power $P \approx 2$ W. In addition, tubes of this type are more convenient because heat is not emitted outside the water-cooling housing in this case, and the protective housing of the laser is not heated.

The results obtained in our experiments with small-scale pulse-periodic cataphoresis He – Sr⁺ laser [28, 29] are of special interest. Cataphoresis has been successfully employed for a long time in continuous-wave ion metal-vapour lasers to ensure a uniform distribution of a vapour along the active length. A He – Cd⁺ laser ($\lambda = 441.6$ and 325 nm) is the most widespread laser of this type. Such a laser, which was first proposed in Ref. [30], was implemented in Refs [31 – 33]. This laser is the most commercially successful among all the metal-vapour lasers. Lasers of this type have gained various important applications [34] due to their simplicity, convenience in exploitation, and the reliability of construction, which is only slightly more complicated than the construction of a He – Ne laser.

In our experiments [28, 29], we employed cataphoresis to deliver a vapour to the active area in pulsed metal-vapour lasers. This approach has never been used in pulse-periodic lasers before, although there were several attempts to employ different types of forced mixture circulation in such lasers [23, 35, 36]. We have demonstrated that the use of cataphoresis in the pulsed regime allows a uniform distribution of a vapour in the active area to be produced. The discharge channel in this case is not blocked by pieces of a

metal, no arc discharge arises on these pieces, and no uncontrollable evaporation occurs. Using this approach, one can independently adjust the energy deposition and the pressure of a metal vapour without using pumps for forced mixture circulation.

To calculate the mean flow rate of a metal vapour due to cataphoresis in the pulse-periodic regime, we can employ the following expression:

$$v = bE_0\tau_p f\theta, \quad (10)$$

where b is the mobility of metal ions; E_0 is the field strength in the current pulse; τ_p is the duration of the discharge current pulse; $\theta = n^+/n$ is the ionisation degree of metal atoms; and n and n^+ are the concentrations of metal atoms and ions, respectively. For typical operation conditions of a He – Sr⁺ laser ($E_0 \approx 1000 \text{ V cm}^{-1}$, $\tau_p \sim 0.1 \text{ } \mu\text{s}$, $f = 5 - 10 \text{ kHz}$ [5, 6], and $b \approx 7.1 \times 10^{-13} \text{ m}^2 \text{ V}^{-1} \text{ s}^{-1}$ [37] for $p_{\text{He}} \approx 0.5 \text{ atm}$ and $\theta \sim 0.5$), formula (10) yields $v = 20 - 40 \text{ cm s}^{-1}$, which is comparable with vapour flow rates in continuous-wave cataphoresis metal-vapour lasers [5, 6].

Provided that a metal vapour is condensed near the cathode, the distribution of a vapour in the continuous-wave regime is described by the following expression [30]:

$$\frac{n}{n_0} = \frac{1 - \exp[\beta(1 - z/l)]}{1 - \exp \beta}, \quad (11)$$

where $\beta = e\theta E_0 l / kT$, z is the coordinate measured along the tube axis, and n_0 is the concentration of the metal vapour in the vaporiser (with $z = 0$).

The field is not applied permanently to a tube in the repetitively pulsed regime. Therefore, the parameter β is given by

$$\beta = \frac{\theta e E_0 l}{kT} \tau_p f. \quad (12)$$

Fig. 2 displays the dependences of n/n_0 on z/l calculated with the use of formula (11) for different β . These results show that a sufficiently uniform distribution of a metal vapour along the channel and a reliable blocking of this vapour from the anode side are achieved with

$$\beta \geq 10. \quad (13)$$

Applying formula (12) for typical operation conditions of a

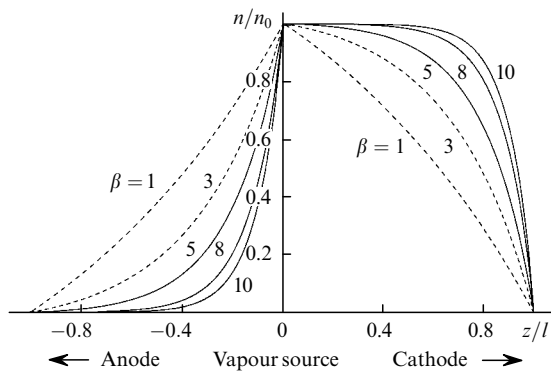


Figure 2. Distribution of the relative concentration of a metal vapour along the discharge tube of a pulse-periodic cataphoresis metal-vapour laser.

repetitively pulsed He – Sr⁺ laser, we find that $\beta = 95 - 190$ (for $l = 26 \text{ cm}$, $T = 870 \text{ K}$), i.e., criterion (13) is satisfied with a large safety margin.

A small-scale glass-ceramic cataphoresis tube 10 (Fig. 1d) with $d = 3 \text{ mm}$ and $l = 26 \text{ cm}$ ($V_a = 1.84 \text{ cm}^3$) was constructed for a He – Sr⁺ laser. Strontium was evaporated in the regime of self-heating in an expanding tube channel ($d_2 \approx 8 \text{ mm}$). The main channel was somewhat overheated in this regime, which prevented the deposition of a strontium vapour in this channel. In these experiments, a uniform distribution of a strontium vapour was achieved for the first time under conditions of cataphoresis gas circulation in the pulse-periodic regime, and lasing on the line with $\lambda = 430.5 \text{ nm}$ was observed. The pressure of helium and the pulse repetition rate were varied within the following ranges: $p_{\text{He}} = 0.3 - 1 \text{ atm}$ and $f = 25 - 50 \text{ kHz}$. Radiation powers $P = 510 \text{ mW}$ and $P_{\text{sp}} = 277 \text{ mW cm}^{-3}$ were achieved with $f = 30 \text{ kHz}$ and $p_{\text{He}} = 0.7 - 0.8 \text{ atm}$. The specific mean radiation power achieved in these experiments is a record value for He – Sr⁺ lasers of all the types (see Table 1). The gain obtained in these experiments, $\kappa_0 = 0.15 \text{ cm}^{-1}$, also corresponds to a maximum value for He – Sr⁺ lasers.

Note that the cataphoresis He – Sr⁺ laser tube is characterised by a comparatively large ratio $d_1/d \approx 3$. In accordance with Eqns (7) and (9), this is one of the factors ensuring high values of P_{sp} and f . This circumstance is illustrated in Fig. 3, which shows that the parameters of most of the tubes presented in the table are satisfactorily approximated with a straight line in the plane of coordinates P_{sp} and d_1/d^2 . The only exception to this rule is associated with a water-cooled tube. The regime of this tube does not correspond to the regime of natural convective and radiative heat transfer under conditions of self-heating.

Thus, the use of cataphoresis allowed the creation of a small-scale, simple, and efficient He – Sr⁺ laser capable of generating radiation with a power $P \approx 0.5 \text{ W}$ in the violet spectral range. We anticipate that a cataphoresis He – Ca⁺ laser may have comparable characteristics.

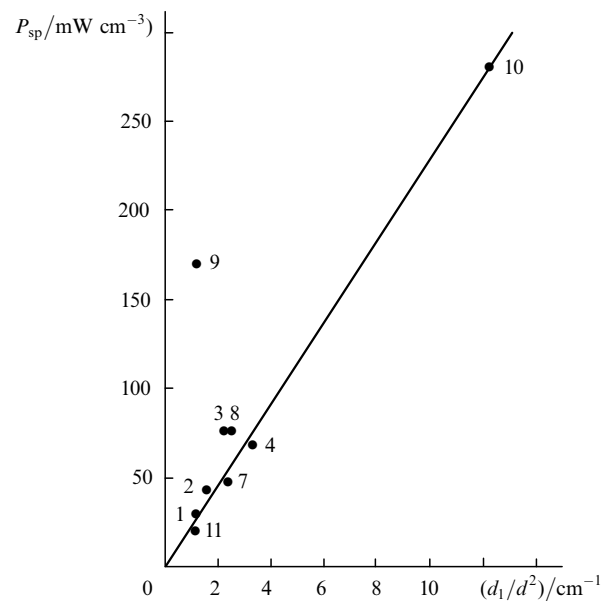


Figure 3. Specific mean power of a He – Sr⁺ (Ca⁺) laser as a function of the ratio d_1/d^2 . The indexing of points corresponds to the table.

Laser radiation powers $P \approx 30 - 50$ mW are sufficient for many applications (this range of radiation powers is typical of He – Cd⁺ lasers). A He – Sr⁺(Ca⁺) laser capable of generating radiation with such powers may have $l \approx 3 - 5$ cm. Consequently, such a laser would require low power-supply voltages, which would make this laser portable and even more convenient. Note also that the cataphoresis method of vapour delivery may offer much promise also for other pulse-periodic metal-vapour lasers, such as copper-vapour, barium-vapour, and copper-bromide-vapour lasers.

4. Applications of small-scale He – Sr⁺(Ca⁺) lasers

Short-wavelength radiation produced by small-scale He – Sr⁺(Ca⁺) lasers may be employed for diversified applications. Below, we discuss some of these possible applications.

Radiation at 430.5 nm and especially radiation at 373.7 nm hold much promise for photolithography in semiconductor microtechnology, since these wavelengths coincide with absorption maxima of the most efficient and widespread photoresists [38]. Because of the same reason, radiation of these lasers is suitable for applications in embossed holography, as the above-mentioned photoresists are employed for the creation and mass production of holograms.

Holographic applications require a high coherence of radiation, which can be achieved with small-scale (especially cataphoresis) He – Sr⁺(Ca⁺) lasers with a small diameter of the discharge channel. A typical bandwidth of radiation produced by these lasers ranges from 0.5 to 1.5 GHz [21]. Hence, the coherence length can be estimated as $\sim 10 - 30$ cm. Our estimates show that, in the efficiency of action on a photoresist, a He – Ca⁺ laser with $P = 0.5$ W is equivalent to an Ar⁺ laser with $P = 10 - 50$ W [6, 39].

Short-wavelength radiation of He – Sr⁺(Ca⁺) lasers can be also employed for cleaning the surfaces of semiconductor plates, trimming parameters of microcircuit components, defect correction, etc. [39].

Violet and ultraviolet radiation is usually preferable in fluorescence and Raman spectroscopy, as well as in chromatography. Such methods of analysis are widely employed in ecology, especially for monitoring characteristics of water resources. Specifically, the wavelength 373.7 nm of CaII coincides with the maximum of absorption and excites fluorescence of most of especially toxic water pollutants — polyaromatic hydrocarbons [40]. Radiation of a strontium laser offers much promise for lidar studies of the atmosphere [41].

In medicine, radiation of a He – Ca⁺ laser at 373.7 nm is well suited for a conservative phototreatment of neonatal jaundice [42, 43] and UV physiotherapy [44]. Radiation at 416.2 and 430.5 nm produced by a He – Sr⁺ laser can be employed for early noncontact diagnosis of diabetes from the fluorescence of eye cornea [45] and for a photodynamic therapy and diagnosis of oncological tumours. Currently, expensive and cumbersome krypton ion lasers are used for this [46, 47]. Recent studies have demonstrated that radiation within the range of wavelengths from 360 to 450 nm with a power $P \approx 20$ mW can be employed for diagnosis and detection of lung cancer without introducing photoscintillators into a patient [48] or using very low doses of such photoscintillators contained, for example, in a glass of orange juice [49].

Lasers of the considered type also hold much promise for

photosensitiser whose absorption band is centred around 420–450 nm. When a tooth is irradiated with light within this wavelength range, healthy enamel fluoresces in the red region at 680 nm, while enamel with early signs of dental caries fluoresces in the green region at 550 nm [49]. Radiation of a He – Sr⁺(Ca⁺) laser can be also employed to solidify ceramics widely used in stomatology. A more detailed review of these and many other applications of the considered lasers (both implemented in practice and considered as promising) is presented in [6–11].

5. Conclusions

Thus, small-scale recombination He – Sr⁺(Ca⁺) lasers, especially their cataphoresis modifications, are simple and efficient sources of violet and UV coherent radiation. We expect that such lasers may gain wide acceptance upon their industrial production and as soon as these lasers become available for consumers and designers of scientific instruments.

Acknowledgements. We are grateful to O O Prutsakov for his help in the preparation of this manuscript. This study was supported in part by the Russian Foundation for Basic Research (project no. 99-02-17539) and the 'Integration' Federal Program (project no. 582).

References

1. Latush E L, Sem M F Zh. Eksp. Teor. Fiz. **64** 2017 (1973) [Sov. Phys. JETP (1973)]
2. Latush E L, Sem M F Kvantovaya Elektron. (Moscow) no. 3 (15) 66 (1973) [Sov. J. Quantum Electron. **3** 216 (1973)]
3. Zhukov V V, Latush E L, Mikhalevskii V S, Sem M F Kvantovaya Elektron. (Moscow) **4** 1249 (1977) [Sov. J. Quantum Electron. **7** 704 (1977)]
4. Zhukov V V, Kucherov V S, Latush E L, Sem M F Kvantovaya Elektron. (Moscow) **4** 1257 (1977) [Sov. J. Quantum Electron. **7** 708 (1977)]
5. Ivanov I G, Latush E L, Sem M F Ionnye Lazery na Parakh Metallov (Metal-Vapour Ion Lasers) (Moscow: Energoatomizdat, 1990)
6. Ivanov I G, Latush E L, Sem M F Metal Vapour Ion Lasers: Kinetic Processes and Gas Discharges (Chichester: John Wiley & Sons, 1996)
7. Little C E Metal Vapour Lasers: Physics, Engineering and Applications (Chichester: John Wiley & Sons, 1999)
8. Latush E L, Sem M F, Bukshpun L M, Koptev Yu V, Atamas' S N Opt. Spektrosk. **72** 1215 (1992) [Opt. Spectrosc. (USSR) (1992)]
9. Latush E L, Sem M F, Koptev Yu V, Bukshpun L M, Atamas' S N Proc. SPIE **2110** 106 (1993)
10. Sem M F, Latush E L, in Pulsed Metal Vapour Lasers, NATO ASI Series, 1. Disarmament Technologies (Dordrecht: Academic, 1996) vol. 5, p. 55
11. Latush E L, Sem M F, Chebotarev G D, in Pulsed Metal Vapour Lasers, NATO ASI Series, 1. Disarmament Technologies (Dordrecht: Academic, 1996) vol. 5, p. 149
12. Latush E L, Sem M F Pis'ma Zh. Eksp. Teor. Fiz. **15** 645 (1972) [Sov. Phys. JETP (1972)]
13. Bokhan P A, Sorokin A R Opt. Quantum Electron. **23** S523 (1991)
14. Bukshpun L M, Atamas' S N, Zhukov V V, Latush E L, Sem M F Izv. Vyssh. Uchebn. Zaved. Ser. Fiz. no. 6 105 (1983) [Sov. Phys. J (1983)]
15. Butler M S, Piper J A Opt. Lett. **12** 166 (1987)
16. Butler M S, Piper J A IEEE J. Quantum Electron. **21** 1536 (1985)
17. Bethel J W, Little C E Opt. Commun. **84** 317 (1991)

18. Bukshpun L M, Latush E L, Sem M F *Kvantovaya Elektron.* (Moscow) **15** 1762 (1988) [*Sov. J. Quantum Electron.* **18** 1098 (1988)]
19. Bukshpun L M, Latush E L, Sem M F *Teplofiz. Vysokikh Temperatur* **24** 402 (1986)
20. Chebotarev G D, Latush E L, *Kvantovaya Elektron.* (Moscow) **30** 393 (2000) [*Quantum Electron.* **30** 393 (2000)]
21. Zhukov V V, Kucherov V S, Latush E L, Sem M F, Tolmachev G N *Pis'ma Zh. Tekh. Fiz.* **2** 550 (1976) [*JETP Lett.* (1976)]
22. Chebotarev G D, Latush E L, Sem M F *J. Moscow Phys. Soc.* **7** 125 (1997)
23. Atamas' S N, Latush E L, Sem M F *J. Russ. Laser Res.* **15** 66 (1994)
24. Butler M S, Piper J A *Appl. Phys. Lett.* **42** 1008 (1983)
25. Butler M S, Piper J A *Appl. Phys. Lett.* **43** 823 (1983)
26. Brundt M *Appl. Phys. Lett.* **42** 127 (1983)
27. Zhukov V V Author's Abstract of Candidate Dissertation (Khar'kov: Khar'kov State University, 1978)
28. Latush E L, Chebotarev G D, Vasilchenko A V *Proc. SPIE* **3403** 141 (1998)
29. Latush E L, Chebotarev G D, Vasilchenko A V *Opt. Atmos. Okeana* **11** 171 (1998)
30. Sosnowski T P *J. Appl. Phys.* **40** 5138 (1969)
31. Goldsborough J P, Hodges E B *IEEE J. Quantum Electron.* **5** 361 (1969)
32. Goldsborough J P *Appl. Phys. Lett.* **15** 159 (1969)
33. Fendley J R Jr, Gorog I, Hernqvist K G, Sun C *IEEE J. Quantum Electron.* **6** 8 (1970)
34. Anderson S G *Laser Focus World* **35** (1) 80 (1999)
35. Bokhan P A, Zakrevskii D E *Kvantovaya Elektron.* (Moscow) **18** 926 (1991) [*Sov. J. Quantum Electron.* **21** 838 (1991)]
36. Loveland D G, Orchard D A, Zerouk A F, Webb C E *Meas. Sci. Technol.* **2** 1083 (1991)
37. Carman R J *IEEE J. Quantum Electron.* **26** 1588 (1990)
38. Veiko V P *Lazernaya Obrabotka Plenochnykh Elementov* (Laser Processing of Film Elements) (Leningrad: Mashinostroenie, 1986)
39. *Laser Lines*, LiCoNIX Quarterly Newsletter no. 2, 1 (1991)
40. Ksenofontova N M, Malevich I A, Chubarov S I *Zh. Prikl. Spektrosk.* **59** 7 (1993) [*J. Appl. Spectrosc. (USSR)* (1993)]
41. Burlakov V D, Zuev V V, Evtushenko G S, et al. *Opt. Atmos. Okeana* **6** 326 (1993)
42. Ppotapenko A Ya. *Sorosovskii Obrazovatel'nyi Zh.* no. 10 13 (1996)
43. Piruzyan L A *Problemy Meditsinskoj Biofiziki* (Problems of Medical Biophysics) (Moscow: Znanie, 1991)
44. Vetchinnikova O N *Laser Market* (4) 14 (1994)
45. Applications unlimited, *Photonics Spectra* **27** (5) 86 (1993)
46. *Spravochnik po Lazernoi Tekhnike* (Handbook of Laser Engineering), Ed. A P Napartovich (Moscow: Energoatomizdat, 1991)
47. Stuart M L *Proc. IEEE* **80** 869 (1992)
48. Grunt B *Biophotonics Intern.* **4** (4) 18 (1997)
49. Marx B R *Laser Focus World* **35** (2) 31 (1999)